Instantaneous normal mode analysis of orientational motions in liquid water: Local structural effects

S. L. Chang, Ten-Ming Wu, and Chung-Yuan Mou

Citation: The Journal of Chemical Physics **121**, 3605 (2004); doi: 10.1063/1.1772759
View online: http://dx.doi.org/10.1063/1.1772759
View Table of Contents: http://scitation.aip.org/content/aip/journal/jcp/121/8?ver=pdfcov
Published by the AIP Publishing

Instantaneous normal mode analysis of orientational motions in liquid water: Local structural effects

S. L. Chang[a] and Ten-Ming Wu[b]
Institute of Physics, National Chiao-Tung University, Hsin Chu 300, Taiwan

Chung-Yuan Mou
Department of Chemistry, National Taiwan University, Taipei 106, Taiwan

(Received 29 March 2004; accepted 20 May 2004)

We have investigated the effects of local structures on the orientational motions in liquid water in terms of the instantaneous normal mode (INM) analysis. The local structures of a molecule in liquid water are characterized by two different kinds of index: the asphericity parameter of its Voronoi polyhedron and the numbers of the H bonds donated and accepted by the molecule. According to the two kinds of index, the molecules in the simulated water are classified into subensembles, for which the rotational contributions to the INM spectrum are calculated. Our results indicate that by increasing the asphericity, the rotational contribution has a shift toward the high-frequency end in the real spectrum and a decrease in the fraction of the imaginary modes. Furthermore, we find that this shift essentially relies on the number of the donated H bonds of a molecule, but has almost nothing to do with that of the accepted H bonds. The local structural effects resulting from the geometry of water molecule are also discussed. © *2004 American Institute of Physics.*
[DOI: 10.1063/1.1772759]

I. INTRODUCTION

Water plays an important role in life processes, industrial applications, and scientific researches, for its abundance and many unusual physical and chemical properties, which are mainly dominated by its hydrogen (H) bonding.[1] The H bonds in water form a network, which is complicated in both static structure and dynamics. In the static structure of ice, each molecule is ideally connected through H bonds with four nearest neighbors to form a network of tetrahedrons; however, in liquid water deviations from the ideal tetrahedron result from distortion due to thermal motions and connection with less than four neighbors.[2] The global pattern of the network has been described by various random models, from the two-state network model[3,4] for the heterogeneity in density to a system of H-bond percolation.[5–7] In dynamics, due to thermal fluctuation and diffusion of molecules, each H bond in water may break and re-form; the breaking and re-forming processes generally follow a nonexponential kinetics.[8] The H-bonded pattern changes in time with the rearrangement of the H-bond connections. In general, water dynamics is influenced by the complex H-bonded network; especially, at the time scale studied by the ultrafast spectroscopy, the dynamics at a molecular level is dominated by the local geometry of the network.

Recently, in terms of the pump-probe technique in a femtosecond experiment for HDO molecules dissolved in liquid D_2O,[9] the orientational dynamics of molecules in liquid water has been investigated through the subensemble of the HDO molecules selected by the pump pulse with frequencies being in a small region in the absorption spectrum of the OH stretch vibration. Due to the sensitivity of the OH stretch vibration on the length of the H bond attaching to the H atom, it is generally believed that the HDO molecules selected by a low-frequency pulse tend to have the OH···O hydrogen bonds in shorter length and those selected by a high-frequency pulse tend to have the hydrogen bonds in longer length.[10,11] The experimental results show that the orientational relaxation of water molecules depends on the pump frequency: a single slow relaxation process was observed for a low-frequency pulse and two relaxation processes, with a fast rate constant less than 1 ps, for a high-frequency pulse. This gives an indication that at the short time scale the orientational motion of a molecule in liquid water is sensitive to the H-bond connection of the molecule at the initial.

On the other hand, via molecular dynamics (MD) simulations, Yeh and Mou[12] have studied the roles of local structures in the relaxation of orientational dynamics in liquid water by classifying the simulated molecules into subensembles of which the local structures are characterized by the asphericity parameter of the Voronoi polyhedra (VP) constructed for the oxygen atoms.[13] For molecules with strongly aspherical VP, their local structures are basically tetrahedral, and their orientational motions, studied by the rotational autocorrelation functions, exhibit only one slow relaxation rate. However, as the VP are more spherical, with their asphericities in the low-value end of the asphericity distribution of the system, the local structures are highly deviated from the tetrahedral structures, and a fast orientational relaxation with time constant ≈1 ps was found. Therefore, the results of both experiment and simulation apparently indicate that the local

[a]Present address: Department of Computer Science and Information Engineering, National Peng-Hu Institute of Technology, Peng-Hu, Taiwan.
[b]Author to whom correspondence should be addressed. Electronic mail: tmw@faculty.nctu.edu.tw

structures have strong effects on the orientational motions in liquid water at a short time scale.

On the theory side, the short-time dynamics of a liquid can be exactly described by the instantaneous normal mode (INM) approach, in which the potential energy surface is harmonically approximated.[14,15] The INMs of a configuration are the eigenmodes of the corresponding Hessian matrix, the second derivatives of the potential energy,[16,17] and the INM density of states (DOS) is obtained by an ensemble average of configurations. One advantage of the INM approach is that the total DOS of the INMs can be separated into branches characterized with different motions by the projection operators, which are determined by the eigenvector components of the Hessian matrix.[18] For example, the total INM DOS of a molecular liquid can be separated into branches dominated by either the translational or the rotational motions of molecules. So far, in terms of the INM approach, there have been many reports on the dynamics of normal and supercooled liquid water[19–25] and other H-bonded liquids.[26–28] Among them, the formalism of projection operator gives fruitful results; however, most studies focus on the contributions due to the translational motions or the vibrations between molecules. In this paper, we generalize the INM projection formalism in another direction for the molecular subensembles of a liquid, in which the molecules are characterized by their local structures. With the generalized projection operators, we investigate the effects of the local structures on the short-time orientational motions in liquid water.

In order to analyze the local structures of the H-bonded pattern, we make two classifications for all molecules in liquid water according to (a) the asphericity of the VP, and (b) the H-bond configuration of a water molecule, which is defined as the numbers of the H bonds donated and accepted by the molecule.[29] The paper is organized as follows: In Sec. II, the two different sets of molecular subensembles are specified with their local structures and described by other characters; the interrelationship between the two sets is also presented. In Sec. III, the INM approach for water model of rigid molecules is briefly summarized. The generalized projection operators and the corresponding INM DOS for molecular subensembles are given. In Sec. IV, based on the projection method, the results of the INM analysis for the orientational motions in liquid water are presented, and the effects of the local structures are discussed. In Sec. V, we give our conclusions.

II. SUBENSEMBLES OF LOCAL STRUCTURE

We have simulated 256 SPC/E water molecules[30] in a cubic box with periodic boundary conditions at density $\rho=1.0\ \mathrm{g\,cm^{-3}}$ and temperature $T=300\ \mathrm{K}$. The Lennard-Jones potential between two oxygens was truncated at half the box length and shifted upward to make the potential and its first derivative continuous at the cutoff. The Coulomb interactions were treated by the Ewald summation. In our simulations, the leap-frog algorithm was used with a time step of 1 fs, and the SHAKE algorithm was also employed to ensure the rigidity of the molecules.[31] After 300 000 time steps from an initial lattice configuration, we started to take data for 100 configurations at every 1000 steps.

We take the energetic definition for a H bond.[5] That is, two molecules are considered to connect with a H bond as the energy between them is less than a cutoff E_{HB}, which is set to be $-12\ \mathrm{kJ\,mol^{-1}}$ in this work. The length r of the H bond is measured as the distance between the H atom of a molecule and the oxygen of the other. With this H-bond definition, the H-bond lengths in our simulated water systems are found to be within a range between 1.45 Å and 3.0 Å. For the OH$\cdots$O angle, the portion of the angle distribution is roughly 70% for the angles larger than $\theta_c=155°$, and reaches 80% as θ_c is released to 150°. Therefore, with this energetic definition, the geometry distributions of the H bonds in our simulated system are not much different from those obtained with another definition.[28]

In the following, based on the local structures, we present two sets of molecular subensemble according to (a) the geometry of the VP and (b) the H-bond configuration of a molecule.

A. Voronoi polyhedra analysis

Through computer simulations, the VP analysis has been widely used for liquid water.[13,32,33] For a particle in a topologically disordered structure, the geometry of the Voronoi polyhedron, which is a generalization of the Wigner-Seitz unit cell in a crystal, characterizes the arrangement of the nearest neighbors of the particle. A dimensionless parameter to measure the geometry of a Voronoi polyhedron is the asphericity parameter,[13] which is defined as

$$\eta=\frac{A^3}{36\pi V^2}, \tag{1}$$

where A and V are the total surface area and volume of the polyhedron, respectively. By this definition, $\eta=1$ for a sphere. As η increases, the geometry of the polyhedron becomes more aspherical. For the ice I_h structure, in which most molecules are in the tetrahedral arrangement, η is equal to 2.25.

We have performed the VP analysis for the oxygens in our simulated water, and the asphericity distribution of the VP has a shape similar as the one of the TIP4P water model at the same temperature.[12] By dividing the whole distribution into four adjacent sections, with their ranges given in Table I, we separated the molecules of a configuration into four groups, indexed as Voronoi group (VG) I to IV with increasing asphericity. Most of the molecules are in VG II and III, and VG I and IV contain only few percentages. To examine the local structures of the molecules in each VG, we present in Fig. 1(a) the oxygen-oxygen radial distribution functions, $g_{oo}(r)$, of the four VGs. The isosbestic points of the four distributions are similar to those obtained from other water models [TIP4P and SPC (Ref. 32)]. We also calculated the length distributions of the H bonds attaching to the molecules in each VG, and the results, shown in Fig. 1(b), clearly indicate that the distribution shifts toward shorter length as the asphericity increases. Similar to the TIP4P model, the strong first peak in the $g_{oo}(r)$ distribution func-

TABLE I. Averaged number fraction $\chi_L=\langle N_L\rangle/N$ and imaginary-mode fractions $\tilde{f}_\nu$ of Voronoi group (VG) L (L=I, II, III, and IV) in liquid water at $\rho=1.0$ g cm^{-3} and $T=300$ K. η is the asphericity range of each VG. $\langle N_L\rangle$ is the averaged number of molecules in VG L and N is the total number of molecules. $\tilde{f}_\nu$ ($\nu=x,y,z$) is the imaginary-mode fraction of the normalized rotational INM spectrum of molecular ν axis.

	Voronoi group I	Voronoi group II	Voronoi group III	Voronoi group IV
η	Below–1.46	1.46–1.72	1.72–1.98	1.98–above
χ_L	0.015	0.6527	0.3168	0.0155
$\tilde{f}_x$	0.223	0.101	0.049	0.032
$\tilde{f}_y$	0.113	0.067	0.044	0.031
$\tilde{f}_z$	0.101	0.043	0.022	0.012

tion of VG IV, and almost four nearest neighbors of each molecule, obtained by integrating $g_{oo}(r)$ up to the first minimum, suggest that in the first shell of the molecules in VG IV the tetrahedral arrangement is the most possible local structure. For VG I, the plateau region within the first minimum in $g_{oo}(r)$ and the longer H-bond length indicate that the molecules in VG I have more random local structures and are more weakly connected through H-bonds with their neighbors than molecules in the other three VG groups. Thus, from the VP analysis, a structural description for the two-state mixture model of liquid water has been proposed.[12] In this description, the local structures of liquid water are described as a mixture of randomly structured patches (VG I) and highly ordered regions (VG IV) immersing in a large pool of water molecules whose asphericites are intermediate between the two regions.

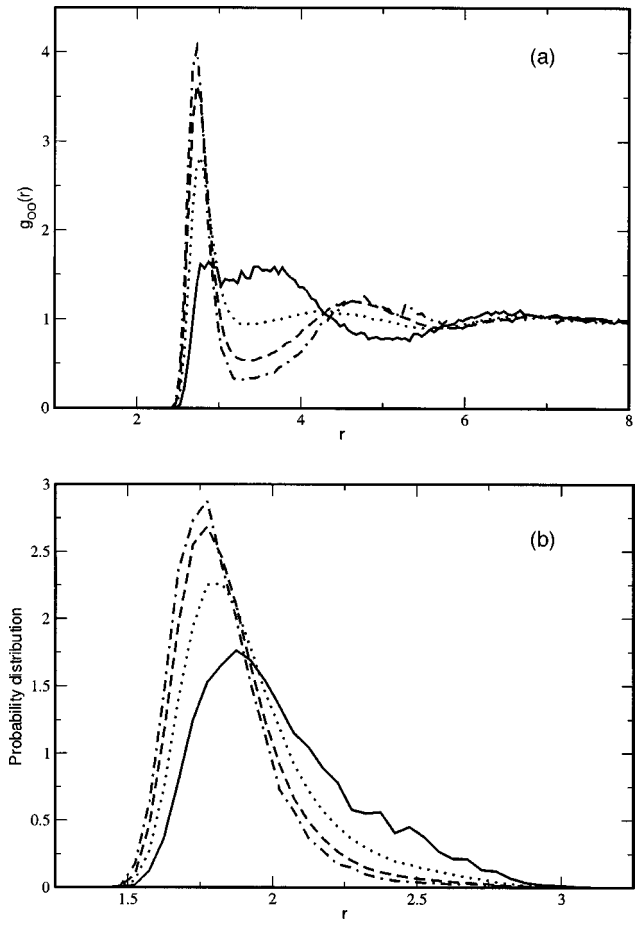

FIG. 1. The oxygen-oxygen radial distribution functions (a) and the distributions of the H-bond length (b) for molecules in Voronoi group (VG) I to IV for liquid water at $\rho=1.0$ g cm^{-3} and $T=300$ K. The solid, dot, dash, and dot-dash lines are for VG I, II, III, and IV, respectively. The unit of distance r is in Å. Each distribution in (b) is normalized to unity.

B. H-bond configurations

Though the VP analysis is a powerful tool for analyzing the local structures of liquid water, it will be helpful for understanding the dynamics of the H-bonded network if more information about the local connections of H bonds can be obtained. Here, we do another classification for molecules in liquid water by the H-bond configuration of a molecule. We employ, for example, the notation D2A1 to denote the H-bond configuration of a molecule donating two H bonds and accepting one. In our simulated systems, we found ten possible H-bond configurations whose averaged number fractions are listed in Table II. Both fractions of molecule with four H bonds and with three H bonds are roughly equal to 40%; our data are somewhat different from those given in Ref. 34 due to the difference in the definition of a H bond. For molecules with two H bonds, it is found that the D1A1 configuration has a much higher probability than the other two configurations, D2A0 and D0A2. Due to the distortion of the H-bonded network, molecules with five H bonds are found in a fraction about 4%, among which the probability for three accepted H bonds is larger than that for three donated H bonds.

Since the processes of breaking and making H bonds frequently occur in liquid water, each H-bond configuration survives with a certain lifetime. For a H-bond configuration, denoted by s, its lifetime can be estimated through the correlation function $C_s(t)$, which is defined as

$$C_s(t)=\frac{\langle h_s(t)h_s(0)\rangle}{\langle h_s^2\rangle}, \tag{2}$$

where $h_s(t)=1$ if the molecule at time t is in the configuration s and $h_s(t)=0$ otherwise. Therefore, $C_s(t)$ is the probability that the molecule is in the H-bond configuration s, given that it was in the same configuration at $t=0$. The correlation functions of several H-bond configurations are shown in Fig. 2. A general feature of these curves is that after a fast transient decay, the curve of $C_s(t)$ has a bump occurring roughly at 0.05 ps, and then follows by a slowly nonexponential decay. The bump, with different amplitude for different H bond configuration, is similar as those observed at the same time scale in the reactive flux correlation functions in the study of H-bond kinetics in liquid water,[8,35] and its physical origin is attributed to the restoration of the H-bond configuration, which changed during the past transient period, to its initial one. The lifetime τ_s of the configuration s is estimated to be the time where $C_s(t)$ reaches 0.5. Listed in Table II are the lifetimes of the ten possible configurations. Generally, the larger the average fraction of a H-bond configutration found in the system at an instant, the longer the

TABLE II. Averaged number fraction $\chi_s=\langle N_s\rangle/N$, lifetime τ_s, and imaginary-mode fraction $\tilde{f}_x$ of H-bond configuration s in liquid water with the cutoff energy of a H bond at -12 kJ mol^{-1}. $\langle N_s\rangle$ is the averaged number of molecules with the H-bond configuration s in a system of total N particles. The lifetime τ_s, in fs, is estimated as described in the text. $\tilde{f}_x$ is the imaginary-mode fraction of the normalized rotational INM spectrum of the molecular x axis.

Config. (s)	D3A2	D2A3	D2A2	D1A2	D2A1	D0A2	D1A1	D2A0	D1A0	D0A1
χ_s	0.006	0.031	0.396	0.169	0.233	0.016	0.12	0.01	0.006	0.013
τ_s	5	10	166	13	20	7	11	6	5	8
$\tilde{f}_x$	0.046	0.023	0.038	0.106	0.042	0.200	0.125	0.044	0.124	0.227

lifetime of the configuration. The D2A2 configuration, which is the most stable H-bonded structure in liquid water, has the longest lifetime, which is estimated to be 150 fs and comparable in order with that given in the other report.[34]

We have presented the results of two analyses for the local structures of liquid water with the same simulated configurations. It is interesting to examine the interrelationship between the VP and the H-bond-configuration analyses. Shown in Fig. 3 is the normalized distribution of the H-bond configuration for molecules in each VG. Several points are worth being noticed. First, for VG IV, the distribution is almost concentrated in the D2A2 configuration, and the probability to find molecules having H bonds less than three is very small. On the other hand, the distribution of VG I behaves quite differently: more spread among different H-bond configurations, with D1A1 being the most probable one. Second, the probability of finding a D2A2 molecule is found to increase with the increase of η (the data are almost 70% molecules in VG IV, but only about 7.5% in VG I), However, the trend is reversed for the probability of finding a D1A1 molecule, with 32% molecules in VG I, and 3.5% in VG IV. These results are consistent with the information obtained from the $g_{oo}(r)$ radial distribution function.

III. INM FORMALISM FOR SUBENSEMBLES

The INM formalism for liquid water of rigid molecules has been given in some details in Ref. 19. Here, we first give a brief summary of the theory and the projection method, and then make a generalization for subensembles of a system.

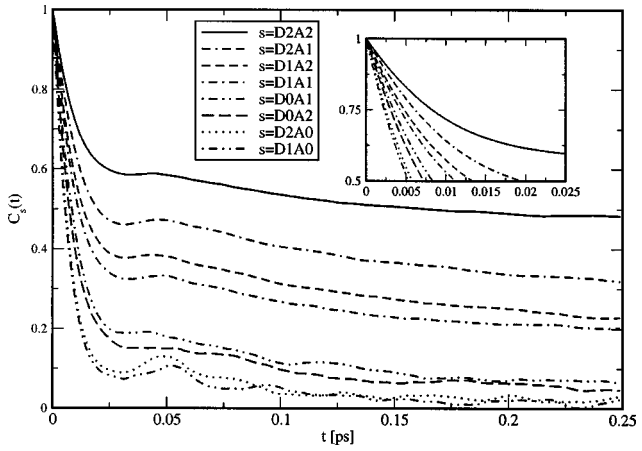

FIG. 2. The time correlation function $C_s(t)$ of H-bond configuration s. The inset shows the decay of $C_s(t)$ in the short-time regime.

For an instantaneous configuration of N rigid water molecules with each mass m, the mass-weighted coordinates of molecule j are defined as $z_{j\mu}=\sqrt{m}\mathbf{r}_j$, for $\mu=1, 2, 3$, where $\mathbf{r}_j$ is the center-of-mass position of molecule j, and $z_{j\mu}=\{\sqrt{I_x}\xi_{jx},\sqrt{I_y}\xi_{jy},\sqrt{I_z}\xi_{jz}\}$ for $\mu=4, 5, 6$, where $I_\nu(\nu=x,y,z)$ is the moment of inertia along the ν principal axis of the molecule. $\{\xi_{jx},\xi_{jy},\xi_{jz}\}$ are the angles of rotation around the direction of the corresponding principal axis of the molecule, which are assumed to be fixed at that instant, with their time derivatives giving exactly the relationship between the three angular velocities along the axes and the time rate of change of the three Euler angles of the molecular frame obtained from reference transformation.[36]

In the mass-weighted coordinates $z_{j\mu}$, the Hessian matrix at a configuration $\mathbf{R}_0$ is defined as

$$D_{j\mu,k\nu}(\mathbf{R}_0)=\left(\frac{\partial^2 V}{\partial z_{j\mu}\partial z_{k\nu}}\right)_{\mathbf{R}_0}. \tag{3}$$

If $\mathbf{U}(\mathbf{R}_0)$ is the matrix that diagonalizes the Hessian matrix $\mathbf{D}(\mathbf{R}_0)$ through an orthogonal transformation, the eigenvalues of the Hessian matrix are given as

$$\omega_\alpha^2(\mathbf{R}_0)=\sum_{j\mu,k\nu} U_{\alpha,j\mu}(\mathbf{R}_0)D_{j\mu,k\nu}(\mathbf{R}_0)U_{\alpha,k\nu}(\mathbf{R}_0). \tag{4}$$

Hence, ω_α is the frequency of the INM α, and $U_{\alpha,j\mu}$ is the corresponding eigenvector component in the direction of the mass-weighted coordinate $z_{j\mu}$.

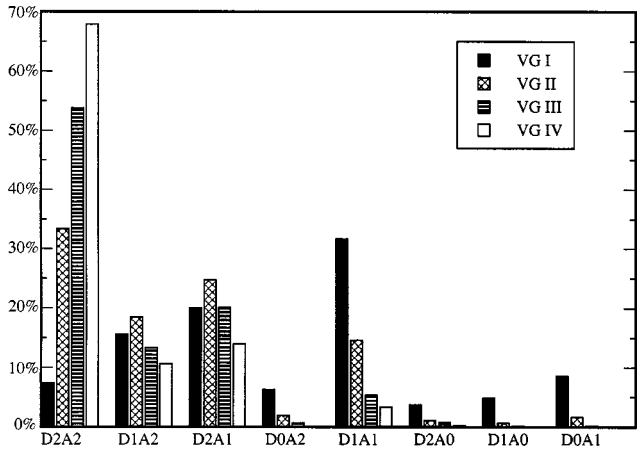

FIG. 3. Percentage distribution of molecules in each Voronoi group (VG) with respect to H-bond configurations. Each distribution is normalized to unity and represented by bars of different symbol: empty for VG IV, line for VG III, cross for VG II, and filled for VG I.

Since both ω_α and $U_{\alpha,j\mu}$ depend on configuration $\mathbf{R}_0$, the total INM DOS is obtained through an ensemble average over configurations, and is written as

$$D(\omega)=\frac{1}{6N}\left\langle \sum_{\alpha=1}^{6N} \delta(\omega-\omega_\alpha(\mathbf{R}_0))\right\rangle, \tag{5}$$

where the angle brackets deonte the average. In principle, $D(\omega)$ includes the contributions from the translational and rotational motions of all molecules. To separate out the two contributions, the projection operators are defined as

$$P_{\alpha\mu}=\sum_{j=1}^{N} U_{\alpha,j\mu}^2 \tag{6}$$

with $\mu=1, 2, 3$ for the center-of-mass motions and $\mu=4, 5, 6$ for the rotational motions. By virtue of the orthonormality of the INM eigenvectors, we have $\Sigma_\mu P_{\alpha\mu}=1$ and $\Sigma_{\alpha=1}^{6N} P_{\alpha\mu}=N$. Thus, the translational contribution to the total DOS is given by

$$D_T(\omega)=\frac{1}{6N}\left\langle \sum_{\alpha=1}^{6N}\sum_{\mu=1}^{3} \delta(\omega-\omega_\alpha)P_{\alpha\mu}\right\rangle, \tag{7}$$

and the contribution due to rotation around a molecular axis is

$$D_\mu(\omega)=\frac{1}{6N}\left\langle \sum_{\alpha=1}^{6N} \delta(\omega-\omega_\alpha)P_{\alpha\mu}\right\rangle, \tag{8}$$

with $\mu=4, 5, 6$ corresponding to the x axis, y axis, and z axis, respectively.

By summing over all molecules, the projection operator $P_{\alpha\mu}$ defined in Eq. (1) is for all species of the system. In the preceding section, we have classified the molecules in the simulated configurations into subgroups according to either the asphericities of their VP or their H-bond configurations. By summing the molecules in each characterized subgroup, the projection operator for each subensemble may be defined. In formalism, this can be done by introducing the selection operators for each subensemble. For example, the selection operator $\Theta_j(L)$ for molecule j in the subensemble of VG L, where L can be I, II, III, and IV, is given as

$$\Theta_j(L)=\begin{cases} 1 & \text{if the asphericity of molecule } j \text{ is} \\ & \text{within the region of VG } L \\ 0 & \text{otherwise.}\end{cases}$$

In terms of the selection operators, the subensemble projection operator of VG L is expressed as

$$P_{\alpha\mu}^L=\sum_{j=1}^{N} U_{\alpha,j\mu}^2\Theta_j(L). \tag{9}$$

Of course, we have the sum rule $P_{\alpha\mu}=P_{\alpha\mu}^{\mathrm{I}}+P_{\alpha\mu}^{\mathrm{II}}+P_{\alpha\mu}^{\mathrm{III}}+P_{\alpha\mu}^{\mathrm{IV}}$. Also, at the configuration $\mathbf{R}_0$, the number of molecules in VG L is given by $N_L=\Sigma_{\alpha=1}^{6N}P_{\alpha\mu}^L$. To avoid the difference in the average number of molecules in each subensemble, we define the normalized rotational INM DOS for the subensemble of VG L as

$$\tilde{D}_\mu^L(\omega)=\left\langle \frac{1}{N_L}\sum_{\alpha=1}^{6N} \delta(\omega-\omega_\alpha)P_{\alpha\mu}^L\right\rangle. \tag{10}$$

$\tilde{D}_\mu^L(\omega)$ is interpreted as the average contribution of a molecule in VG L to the rotational INM spectrum $D_\mu(\omega)$. Therefore, we have

$$D_\mu(\omega)=\frac{1}{6}\sum_{L=\mathrm{I,II,III,IV}} \chi_L\tilde{D}_\mu^L(\omega), \tag{11}$$

where χ_L is the average number fraction of VG L and their values are given in Table I.

Similarly, for the subensemble of the H-bond configuration s, the normalized rotational INM spectrum is defined as

$$\tilde{D}_\mu^s(\omega)=\left\langle \frac{1}{N_s}\sum_{\alpha=1}^{6N} \delta(\omega-\omega_\alpha)P_{\alpha\mu}^s\right\rangle, \tag{12}$$

where $P_{\alpha\mu}^s=\Sigma_{j=1}^{N}U_{\alpha,j\mu}^2\Theta_j(s)$ is the corresponding projection operator, with the selection operator $\Theta_j(s)=1$ if molecule j is in the configuration s and zero otherwise, and N_s is the number of molecules in the H-bond configuration s at configuration $\mathbf{R}_0$.

IV. RESULTS AND DISCUSSIONS

In this section, we present the INM spectrum of liquid water and the various contributions from molecules in different subensembles, with our focus on the rotational contribution. We also compare the rotational contributions of the INM spectrum with the three Gaussian components in the librational region of the recently reported Raman spectrum of liquid water at $T=295\,\mathrm{K}$ and high pressure.[37] The body frame of a water molecule is shown in the inset of Fig. 4, in which the x, y, and z axis have the A_2, B_1, and B_2 symmetry of a C_{2v} molecule, respectively.[38] With the assigned molecular frame and the SPC/E model, the moments of inertial of a water molecule along each of the three principal axes are $I_x=2.216$, $I_y=0.984$, and $I_z=3.20\times10^{-40}\,\mathrm{g\,cm^2}$.

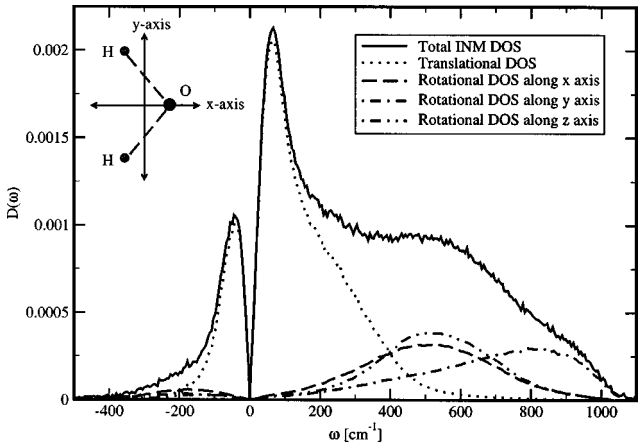

FIG. 4. The total INM DOS of liquid water and its translational and rotational contributions. The rotational contribution is further divided into components around each of the three inertial principal axes shown in the inset in which the center of mass is located at the origin, the oxygen is on the x axis, and the line joining the two hydrogens is parallel to the y axis.

The total INM DOS of liquid water and the translational and rotational contributions are presented in Fig. 4. Compared with the results given in Ref. 19 in which the TIPS2 model was calculated, the total INM DOS calculated with the SPC/E model is similar in the spectrum shape, except for a larger fraction in the imaginary branch (about 12%). The projection method clearly shows that the low-frequency parts (roughly less than 300 cm^{-1} in the real branch and 200 cm^{-1} in the imaginary branch) are dominated by the translational motions. The physical origin of the strong peak near 70 cm^{-1} in the real-frequency spectrum is attributed to the oxygen-oxygen-oxygen bending motions; more details are given in Ref. 28.

The rotational contribution has been divided into components around each of the three inertial principal axes of a water molecule. For the real-frequency branch, the spectrum shape of the y axis is highly asymmetric and has a peak position near 830 cm^{-1}; the peak position is the largest one among the three components since I_y is the smallest one among the three moments of inertia. For the x and z axis, the real-frequency spectra can be fit by a Gaussian function $D_{\mathrm{fit}}(\omega)=A\exp\{-(\omega-\omega_0)^2/2\sigma^2\}$ with the mean frequency $\omega_{0x}=500\,cm^{-1}$ and $\omega_{0z}=530\,cm^{-1}$ and the width $\sigma_x=193\,cm^{-1}$ and $\sigma_x=164\,cm^{-1}$, respectively. Though I_x and I_z are different, the almost equivalence in the rotational spectrum for the two axes is explained by the compensation in the intermolecular interactions.[19] As compared with the three Gaussian components in Raman spectrum of liquid water with maxima at 430, 630, and 795 cm^{-1}, which are interpreted as the librations in the liquid phase corresponding to the rotations with the A_2, B_2, and B_1 symmetry of a water molecule in the gas phase, respectively, one can naturally find the correspondence between the INM rotational component of the y axis and the component with maximum at 795 cm^{-1} in the Raman spectrum; however, there is no clear correspondence between the two spectra for the other two components.

By further subdividing the rotational component of each molecular axis into the contributions from the four subensembles of VG, the normalized rotational INM spectrum of each subensemble is presented in Fig. 5, from which some general features related to the local structures are clearly evidenced. For each molecular axis, as the asphericity of the Voronoi polyhedron increases, the mean frequency of the real-frequency spectrum shifts toward the high-frequency end, and the imaginary-mode fraction $\tilde{f}_\nu(\nu=x,y,z)$, which is the area under the normalized rotational INM spectrum in the imaginary branch, decreases. With the data given in Table I for $\tilde{f}_\nu$ of the four VG subensembles, we find that the relation $\tilde{f}_x>\tilde{f}_y>\tilde{f}_z$ is valid for all of the VG subensembles, with $\tilde{f}_y$ being much closer to $\tilde{f}_x$ for VG III and IV but to $\tilde{f}_z$ for VG I. The differences among $\tilde{f}_x$, $\tilde{f}_y$, and $\tilde{f}_z$ indicate that the rotational motions of molecules in liquid water are anisotropic in the short-time scale, as other analysis has pointed out.[39] The order of the three quantities is generally determined by two factors: the symmetry of the molecular axis and the local structures of a water molecule. For a single molecule, the x axis is a twofold axis of symmetry under rotation. That is, rotating a molecule alone by 180° about this axis produces the same configuration, so that the potential energy associated with the single-molecule rotations around this axis is double degenerated. Therefore, $\tilde{f}_x$ is expected to be larger than $\tilde{f}_y$ and $\tilde{f}_z$. However, the symmetry of the axis can be destroyed by the local structure of a molecule, especially by the H-bond configuration, which is discussed in the following paragraph.

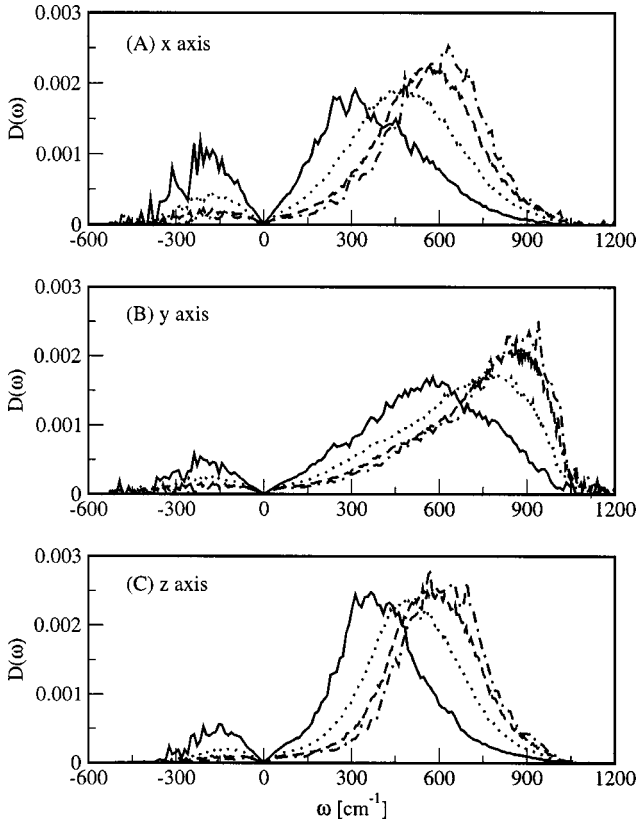

FIG. 5. The normalized rotational INM spectra of the molecular x axis (a), y axis (b), and z axis (c) for each Voronoi group (VG). For all panels, the solid lines are for VG I, the dot lines for VG II, the dash lines for VG III, and the dot-dash lines for VG IV.

More interesting information can be obtained from the normalized rotational INM spectra for the subensembles of different H-bond configurations. The results for the molecular x axis, which is along the direction of dipole moment, are presented in Fig. 6. The important information from Fig. 6 is that the rotational INM spectrum essentially depends on the number of the donated H bonds of a molecule, but has almost nothing to do with that of the accepted H bonds; similar results are also observed in the spectra of the other two molecular axes. This can be realized as that by exerting relatively smaller torques due to the closeness in position between the center of mass and the oxygen of a water molecule, the accepted H bonds of a molecule play only a minor role in governing the instantaneous rotations of the molecule and, therefore, give no apparent effects on the rotational INM spectrum. On the other hand, the variation of the rotational INM spectrum with increasing the number of the donated H bonds behaves similarly as the change of the spectrum with the increase in the asphericity of Voronoi

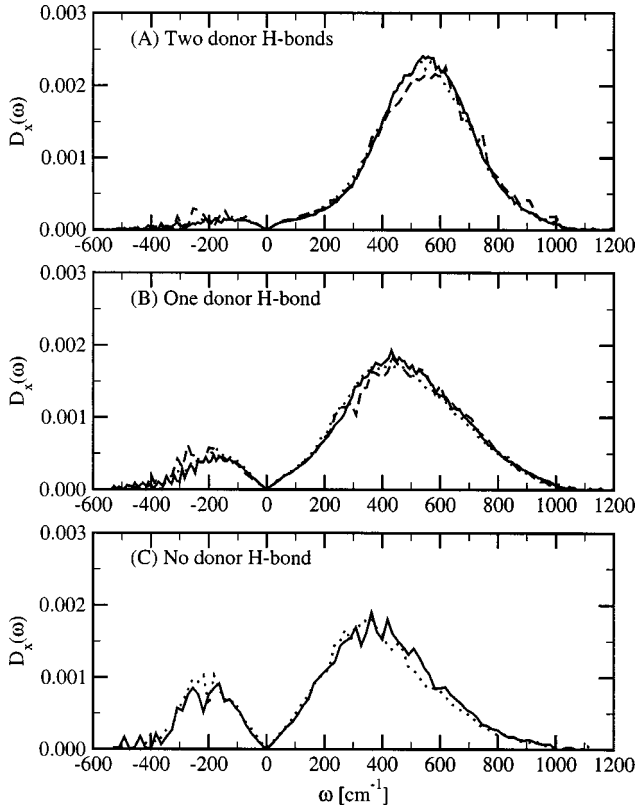

FIG. 6. The normalized rotational INM spectrum of the molecular *x* axis for each H-bond configuration. The three panels are classified for configurations with two (a), one (b), and zero (c) donated H-bonds. In each panel, the solid, dot, and dash lines are for configurations with two, one, and zero accepted H bonds, respectively.

polyhedron mentioned above. Therefore, the results shown in Fig. 6 reflect the structural analyses given in Sec. II: the larger the asphericity of the Voronoi polyhedron of a molecule, the higher the probability for the molecule having two donated H bonds (roughly 80% for VG IV, 70% for VG III, 50% for VG II, and 20% for VG I). In a recent study of HDO rotations in liquid HDO/D_2O solution, a coupling between HDO rotations and the motions of the OH···O hydrogen bond, which is a donated one to HDO, has been indicated.[40] Thus, the coupling between molecular rotations and the motions of the donated H bonds in liquid water is considered as the root cause for the shift of the INM spectrum with the number of the donated H bonds.

For the results given above in regard to the rotational INM spectrum, we give an interpretation from the point of view of potential energy surface.[25,41,42] Generally speaking, the instantaneously rotational motions of the molecules with strongly aspherical local structures are hindered by the H bond connection with their neighbors, so that the profiles of the potential energy surface along most of the rotational degrees of freedom of these molecules are considered to be deep wells with large and positive local curvatures, which cause a large mean value and a rareness in the imaginary modes in the contributed rotational INM spectrum. On the other hand, for species whose local structures are more spherical, the weak connection in H bonds with their neighbors allows the molecules to make either hindered rotations with larger amplitudes or even a rotational diffusion, so that the corresponding profiles are shallower wells or energy barriers for some degrees of freedom, which cause a smaller mean value of the contributed rotational spectrum and a larger fraction of the imaginary modes.

V. CONCLUSION

In this paper, we have investigated the effects of local structure on the contribution of rotational motions to the INM spectrum of liquid water. We characterize the local structures of liquid water by two different kinds of index: the asphericity parameter of Voronoi polyhedron constructed for the oxygen atoms, and the H bond configuration, which is defined as the numbers of the H bonds donated and accepted by a molecule. There is an interrelationship between these two kinds of structural classifications for liquid water. The local structures with high asphericities are more tetrahedral-like, and the corresponding molecules are, generally, connected by two donated and two accepted H bonds. On the other hand, molecules with local structures of low asphericities are diversified in the H-bond configuration, with the configuration of one donated and one accepted H bonds being the most probable one (only about 30%).

According to the indices of local structures, we divide the simulated water molecules into subensembles in two different ways. In one way, by dividing the whole asphericity distribution of the system into four adjacent sections, the molecules are separated into four corresponding subensembles; in the other way, the molecules of the same H-bond configuration are grouped together. In terms of the projection approach, we have separated the rotational contributions around each of the three inertial principal axes into components due to different subensembles. By examining the variations of these rotational components with the asphericity and with the H-bond configuration, we have shown that in liquid water the local structures of the H-bonded network indeed have strong effects on the rotational INM spectrum, which describes exactly the short-time rotational motions.

For all of the three principal axes of water molecule, an increase of the asphericity results in an overall shift of the rotational INM spectrum, indicated by an increase in the mean frequency of the real-frequency branch and a decrease in the fraction of the imaginary modes. Furthermore, we find that it is the number of the donated H bonds of a molecule, rather than that of the accepted H bonds, that is a crucial factor to determine the amount of the shift. Thus, for a molecule in liquid water, within the lifetime of its H-bond configuration, which may be a few femtoseconds or more than a hundred, the H-bond configuration, determined by a few nearest neighbors of the molecule, plays a dominant role in the orientational motions of the molecule at a molecular level, while the effects of other neighboring molecules are expected to come in beyond the lifetime.

For the potential energy surface of liquid water, the profiles along the rotational degrees of freedom of those molecules with highly aspherical local structures are extremely stable so that the associated orientational motions of these molecules are much hindered and more like a librational one. On the contrary, making an essential contribution to the

imaginary INMs through rotations, the molecules with local structures at the low-value end of the asphericity distribution are expected to rotationally diffuse much easier than the molecules at the high-value end of the distribution. Our data also show that no matter what the local structures are, the rotational motions around the dipole moment of a water molecule contribute more to the imaginary INMs than the rotations around any of the other two molecular axes; this is possibly due to the twofold symmetry under rotation around the dipole moment. Therefore, this result suggests a higher probability for rotational diffusion around the dipole moment of a water molecule.

In terms of the projection approach of the INM formalism, we have explored the local structural effects on the orientational motions in liquid water along the three inertial principal axes. More interesting information is expected by extending the exploration to the orientational motions around an OH bond of a water molecule, and the exploration is underway.

ACKNOWLEDGMENTS

We thank Dr. Y. L. Yeh for helping in computer programs of our MD simulations. Also, T.M.W. acknowledges support from the National Science Council of Taiwan, ROC under Grant No. NSC 92-2112-M009020.

[1] F. Franks, *Water: A Comprehensive Treatise* (Plenum, New York, 1972), Vols. 1–7.
[2] F. Sciortino, A. Geiger, and H. E. Stanley, Nature (London) **354**, 218 (1991).
[3] M. Vedamuthu, S. Singh, and G. W. Robinson, J. Phys. Chem. **98**, 2222 (1998); **98**, 8591 (1998).
[4] G. W. Robinson, C. H. Cho, and J. Urquidi, J. Chem. Phys. **111**, 698 (1999); J. Urquidi, S. Singh, C. H. Cho, and G. W. Robinson, Phys. Rev. Lett. **83**, 2348 (1999).
[5] A. Geiger, F. H. Stillinger, and A. Rahman, J. Chem. Phys. **70**, 4185 (1979).
[6] H. E. Stanley and J. Teixeira, J. Chem. Phys. **73**, 3404 (1980).
[7] R. Lamanna, M. Delmelle, and S. Cannistraro, Phys. Rev. E **49**, 2841 (1994).
[8] A. Luzar and D. Chandler, Nature (London) **379**, 55 (1996).
[9] S. Woutersen, U. Emmerichs, and H. J. Bakker, Science **278**, 658 (1997); H. J. Bakker, S. Woutersen, and U. Emmerichs, Chem. Phys. **258**, 233 (2000); H. K. Nienhuys, R. A. van Santen, and H. J. Bakker, J. Chem. Phys. **112**, 8487 (2000).
[10] G. M. Gale, G. Gallot, F. Hache, N. Lascoux, S. Bratos, and J.-Cl. Leicknam, Phys. Rev. Lett. **82**, 1068 (1999).
[11] C. P. Lawrence and J. L. Skinner, J. Chem. Phys. **118**, 264 (2003).
[12] Y. L. Yeh and C. Y. Mou, J. Phys. Chem. B **103**, 3699 (1999).
[13] G. Ruocco, M. Sampoli, and R. Vallauri, J. Mol. Struct. **250**, 259 (1991); G. Ruocco, M. Sampoli, and R. Vallauri, J. Chem. Phys. **96**, 6167 (1992); R. Ruocco, M. Sampoli, A. Torcini, and R. Vallauri, *ibid.* **99**, 8095 (1993).
[14] R. M. Stratt, Acc. Chem. Res. **28**, 201 (1995).
[15] T. Keyes, J. Phys. Chem. A **101**, 2921 (1997).
[16] T. M. Wu and R. F. Loring, J. Chem. Phys. **97**, 8568 (1992).
[17] Y. Wan and R. M. Stratt, J. Chem. Phys. **100**, 5123 (1994).
[18] M. Buchner, B. M. Ladanyi, and R. M. Stratt, J. Chem. Phys. **97**, 8522 (1992).
[19] M. Cho, G. R. Fleming, S. Saito, I. Ohmine, and R. M. Stratt, J. Chem. Phys. **100**, 6672 (1994).
[20] F. Sciortino and P. Tartaglia, Phys. Rev. Lett. **78**, 2385 (1997).
[21] J. T. Kindt and C. A. Schmuttenmaer, J. Chem. Phys. **106**, 4389 (1997).
[22] S. Saito and I. Ohmine, J. Chem. Phys. **108**, 240 (1998).
[23] H. Ahlborn, X. Ji, B. Space, and P. B. Moore, J. Chem. Phys. **111**, 10622 (1999); H. Ahlborn, B. Space, and P. B. Moore, *ibid.* **112**, 8083 (2000).
[24] E. La Nave, A. Scala, F. W. Starr, H. E. Stanley, and F. Sciortino, Phys. Rev. Lett. **84**, 4605 (2000); E. La Nave, A. Scala, F. W. Starr, H. E. Stanley, and F. Sciortino, Phys. Rev. E **60**, 036102 (2001).
[25] H. E. Stanley, S. V. Buldyrev, N. Giovambattista, E. La Nave, A. Scala, F. Sciortino, and F. W. Starr, Physica A **306**, 230 (2002).
[26] G. Garberoglio and R. Vallauri, Phys. Rev. Lett. **84**, 4878 (2000).
[27] G. Garberoglio and R. Vallauri, J. Chem. Phys. **115**, 395 (2001).
[28] G. Garberoglio and R. Vallauri, Physica A **314**, 492 (2002); G. Garberoglio, R. Vallauri, and G. Stumann, J. Chem. Phys. **117**, 3278 (2003).
[29] S. Myneni *et al.*, J. Phys.: Condens. Matter **14**, L213 (2002).
[30] H. J. C. Berendsen, J. R. Grigera, and T. P. Straatsma, J. Phys. Chem. **91**, 6269 (1987).
[31] M. P. Allen and D. J. Tildesley, *Computer Simulation of Liquids* (Clarendon, Oxford, 1987).
[32] J. P. Shih, S. Y. Sheu, and C. Y. Mou, J. Chem. Phys. **100**, 2202 (1994).
[33] P. Jedlovszky, J. Chem. Phys. **111**, 5979 (1999); **113**, 9113 (2000).
[34] G. Sutmann and R. Vallauri, J. Mol. Liq. **98–99**, 213 (2002).
[35] A. Luzar and D. Chandler, Phys. Rev. Lett. **76**, 928 (1996).
[36] H. Goldstein, *Classical Mechanics*, 2nd ed. (Addison-Wesley, New York, 1980).
[37] D. M. Carey and G. M. Korenowski, J. Chem. Phys. **108**, 2669 (1998).
[38] J. M. Hollas, *High Resolution Spectroscopy* (Butterworths, London, 1982), Chap. 5.
[39] J. Ropp, C. Lawrence, T. C. Farrar, and J. L. Skinner, J. Am. Chem. Soc. **123**, 8047 (2001).
[40] G. Gallot, S. Bratos, S. Pommeret, N. Lascoux, J.-Cl. Leicknam, M. Kozinski, W. Amir, and G. M. Gale, J. Chem. Phys. **117**, 113901 (2002).
[41] S. D. Bembenek and B. B. Laird, Phys. Rev. Lett. **74**, 936 (1995).
[42] W. Li, T. Keyes, and F. Sciortino, J. Chem. Phys. **108**, 252 (1998).